The Role of β-effect and a Uniform Current on Tropical Cyclone Intensity

DUAN Yihong*[1,2] (端义宏), WU Rongsheng[1] (伍荣生), YU Hui[2] (余 晖),
LIANG Xudong[2](梁旭东), and Johnny C L CHAN[3] (陈仲良)

[1] *Department of Atmosphere Science, Nanjing University, Nanjing* 210008

[2] *Shanghai Typhoon Institute, Shanghai* 200030

[3] *Dept. of Physics and Materials Science, City University of Hong Kong, Hong Kong*

(Received 17 January 2003; revised 18 September 2003)

ABSTRACT

A limited-area primitive equation model is used to study the role of the β-effect and a uniform current on tropical cyclone (TC) intensity. It is found that TC intensity is reduced in a non-quiescent environment compared with the case of no uniform current. On an f-plane, the rate of intensification of a tropical cyclone is larger than that of the uniform flow. A TC on a β-plane intensifies slower than one on an f-plane. The main physical characteristic that distinguishes the experiments is the asymmetric thermodynamic (including convective) and dynamic structures present when either a uniform flow or β-effect is introduced. But a fairly symmetric TC structure is simulated on an f-plane. The magnitude of the warm core and the associated subsidence are found to be responsible for such simulated intensity changes. On an f-plane, the convection tends to be symmetric, which results in strong upper-level convergence near the center and hence strong forced subsidence and a very warm core. On the other hand, horizontal advection of temperature cancels part of the adiabatic heating and results in less warming of the core, and hence the TC is not as intense. This advective process is due to the tilt of the vortex as a result of the β-effect. A similar situation occurs in the presence of a uniform flow. Thus, the asymmetric horizontal advection of temperature plays an important role in the temperature distribution. Dynamically, the asymmetric angular momentum (AM) flux is very small on an f-plane throughout the troposphere. However, the total AM exports at the upper levels for a TC either on a β-plane or with a uniform flow environment are larger because of an increase of the asymmetric as well as symmetric AM export on the plane at radii >450 km, and hence there is a lesser intensification.

Key words: β-effect, uniform current, asymmetric structure, tropical cyclone intensity change

1. Introduction

The skill of tropical cyclone (TC) motion forecasting has significantly improved in past decades, however the forecasting of TC intensity still needs great effort towards improvement (Elsberry et al., 1992). This is due partially to insufficient observation data and to poor understanding of the mechanism of TC intensity change. Recently, many studies have been made on the effect of vertical shear of the environmental uniform flow on TC intensity (e.g., Shapiro, 1992; Jones, 1995; DeMaria, 1996; Bender, 1997; Holland and Wang, 1999; Peng et al., 1999; Ritchie and Elsberry, 2001; and Frank and Ritchie, 2001). However, the fundamental physical processes of these effects on TC intensity are still not clearly understood. This is the major motivation of the present study.

Past researches have suggested that changes in the planetary vorticity, uniform flow, and vertical wind shear will result in concomitant changes in TC intensity. Madala and Piacsek (1975) showed that a TC in a three-level model intensified at different rates on an f-plane and on a β-plane before the storm stage, but afterwards, the rates were the same. They also found that the intensity of the simulated TC depended heavily on the magnitude of the vertical shear of the basic flow. They hypothesized that the displacement due to

*E-mail: duanyh@mail.typhoon.gov.cn

the β-effect results in the advection of part of the released latent heat out of the region of low-level convergence, and hence in the generation of a weaker warm core in the middle and upper troposphere than its f-plane counterpart. This then results in a less intense TC. The same rate of intensification after the storm stage is due to the slower movement of the TC. Their results seem to suggest that changes in TC intensity are related to its movement although no further evidence was presented. On the other hand, DeMaria and Schubert (1984) found that the intensification rate is very similar on either an f- or a β-plane until 48 h. After this time, the intensity of the TC on the β-plane begins to level off, while that on the f-plane continues to intensify. They argued that it is more difficult to establish a concentrated area of cyclonic rotation in the upper layer through momentum transport in the β-plane case. This is because the center of the upper-layer vortex does not always remain directly over the lower-layer vortex due to the differential advection of the earth's vorticity. Khain (1988) also obtained a similar result. Peng et al. (1999) hypothesized that for a TC on a β-plane or embedded in a uniform flow effect, the area of strongest convergence does not correspond to the area of largest moisture so that convection is less strong compared with the f-plane or no uniform flow case. As a result, the rate of intensification is slower.

These contradictory results suggest that the physical processes responsible for the rate of TC intensification have not been thoroughly examined. Even the most basic question of why or whether TC intensification rates are different on an f- and a β-plane has not been properly answered. The mechanism for the apparently counter-intuitive result that uniform currents from different directions cause TCs to intensify at different rates needs to be identified. These form the objective of the present study.

Section 2 gives a brief description of the numerical model and introduces the initial conditions. The numerical experiments to be conducted are also listed in this section. The intensity changes of TCs embedded in a uniform flow environment and on a β-plane are examined in section 3. The corresponding structure changes are presented in section 4. Based on these results, the physical mechanisms responsible for the different intensity changes are proposed. Further supporting evidence of these mechanisms is given in section 5 in which the angular momentum transports are calculated. Summary of the results and the concluding remarks are presented in section 6.

2. Numerical model and initial conditions

The same as Chan et al. (2001), the Penn State/NCAR (National Center for Atmospheric Research) mesoscale model version 4 (MM4), details of which have been outlined in Anthes et al. (1987), is used for this study. It is a primitive-equation model formulated on a Lambert projection and in σ coordinates, with 15 levels in the vertical. The σ levels are placed at values of 1.0, 0.98, 0.95, 0.90, 0.8, 0.65, 0.5, 0.4, 0.32, 0.26, 0.20, 0.15, 0.10, 0.06, 0.03, and 0.0. The Kuo cumulus parameterization (Kuo 1974; Anthes, 1977) scheme is used. A bulk aerodynamic model of the planetary boundary layer following Deardorff (1972) is employed in which horizontal diffusion is second-order and vertical diffusion is parameterized with K-theory.

Many methods for inserting a vortex into the initial fields have been designed (e.g., Kurihara et al., 1993; Heming et al., 1995; Hodur, 1997). The bogus TC used in the present study is specified by the radius of 15 m s^{-1} (R_{15}) winds, the boundary radius of the TC ($R_{\rm e}$), and the central pressure $P_{\rm c}$. The sea-level pressure at a distance r from the TC center, $P_{\rm se}(r)$, is given by Fujita's (1952) formula:

$$P_{\rm se}(r) = P_{\rm e} - \Delta P \left[1 + \left(\frac{r}{R_0}\right)^2\right]^{-0.5},$$

where $P_{\rm e}$ is the environmental pressure, R_0 the radius of maximum wind, and $\Delta P = P_{\rm e} - P_{\rm c}$.

The model domain is 5000 km×5000 km with a horizontal grid size of 50 km. The "Arakawa B" horizontal grid structure is used. An explicit time-integration scheme developed by Brown and Campana (1978) is employed, which allows for a time step of 60 s, about 1.6 times larger than that allowed by a conventional leapfrog scheme but produces virtually identical results. The inflow/outflow lateral boundary conditions are used. In the vertical, vertical velocity is zero at σ=0 and 1. The domain is large enough so that the boundary conditions should have very little effect on predictions up to 48 h. All the variables are defined at the half-σ levels except vertical velocity.

The control experiment is conducted with a prespecified vortex and a quiescent atmospheric environment. The atmosphere is homogeneous at the standard pressure levels (1000, 850, 700, 500, 300, 200, and 100 hPa). The vertical temperature structure is obtained from the ECMWF (European Centre for Medium-Range Weather Forecast) (10°–20°N, 135°–155°E) reanalysis data (0000 UTC 21 September 1990)

Table 1. List of experiments.

Experiment name	Description
Basic experiment (Expt. F)	Defined as the same as that of Chan et al. (2001) but taking the Coriolis parameter as constant and sea surface temperature as 28°C
Expt. E	Same as Expt. F but with an easterly mean flow (5 m s^{-1})
Expt. B	Same as Expt. F but with a variable Coriolis parameter

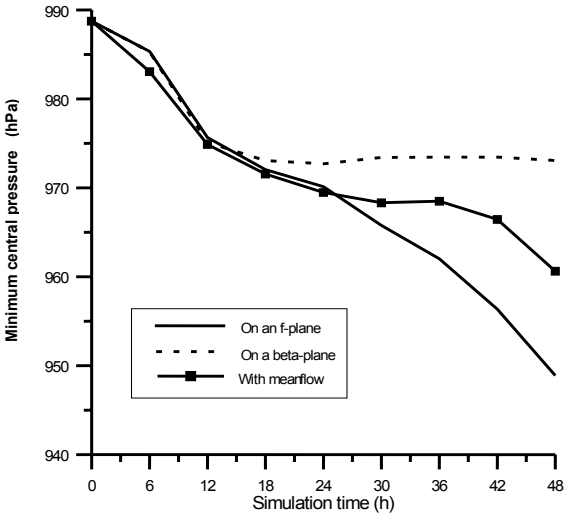

Fig. 1. Time series of minimum central pressure for experiments on an f-plane without uniform flow (solid), on a β-plane without uniform flow (dashed), and with an easterly (squares) uniform flow and on an f-plane.

averaged within 135°–155°E and 10°–20°N. Because the humidity values from the ECMWF reanalysis are too dry for the model TC to grow, these values are set to 90%, 85%, 80%, 50%, 20%, 20%, and 10% at the standard pressure levels from 1000 to 100 hPa, respectively. The geopotential heights at various pressure levels are calculated using the hydrostatic relationship. When an environmental uniform flow is considered, the geopotential height is calculated by geostrophic balance at the pressure levels. To make sure that the uniform flow does not change much during the integration, a preliminary experiment with only a uniform flow was performed up to 48 h. The results suggest that the characteristics of the uniform current were well maintained throughout the integration. The model SST (lower boundary condition) is assumed to be homogeneous at 28°C.

A basic experiment (Expt. F, see Table 1) is first run to produce a realistic TC. Its initial parameters are the same as Expt. A0 of Chan et al. (2001) except the Coriolis parameter is set as constant with a value equal to that at 20°N.

Three experiments performed in this study are listed in Table 1. Experiment F and Expt. E are designed for a TC in a quiescent atmosphere and in easterly uniform flow, respectively. The other experiment (Expt. B) is one with a variable Coriolis parameter but in a quiescent atmosphere.

3. Basic results

3.1 *Changes in TC intensity*

Similar to the results of Peng et al. (1999), the intensification rate for a TC on a β-plane or one embedded in a uniform flow is less than that on an f-plane (Fig. 1). After the adjustment time, the TC on the -plane stops intensifying. By 48 h, the minimum sea-level pressure (MSLP) difference between the f- and the β-plane experiments is about 25 hPa. The corresponding difference in maximum winds is 10 m s^{-1} (42 vs. 32 m s^{-1}). By 48 h, the MSLP is about about 12 hPa higher (maximum winds 4 m s^{-1} less) than that in the f-plane experiment.

3.2 *The horizontal and vertical structures*

As might be expected, a fairly symmetric structure of a TC is simulated in Expt. F (Fig. 2a) since no mechanism exists that can result in an asymmetric structure when the TC is on an f-plane within a quiescent atmosphere. This result is similar to that of Peng et al. (1999).

The horizontal wind distribution, however, becomes asymmetric for a TC embedded in a uniform easterly flow (Fig. 2b). As expected, the maximum wind is located to the north of the TC center due to a superposition of the easterly flow and the TC circulation. Note that the maximum wind is weaker than that in the f-plane simulation. However, the asymmetry in the TC structure is even more pronounced in the β-plane simulation (Fig. 2c), with the maximum wind to the east of the TC.

The vertical motion also shows a fairly symmetric feature in the f-plane simulation (figure not shown). Comparing this with the results for the β-plane and uniform easterly flow experiments, the differences can be clearly identified. First, the main vertical motion is generally confined within 200 km from the TC center in the f-plane case, but in the easterly flow case, this range is extended to about 300 km and the width of

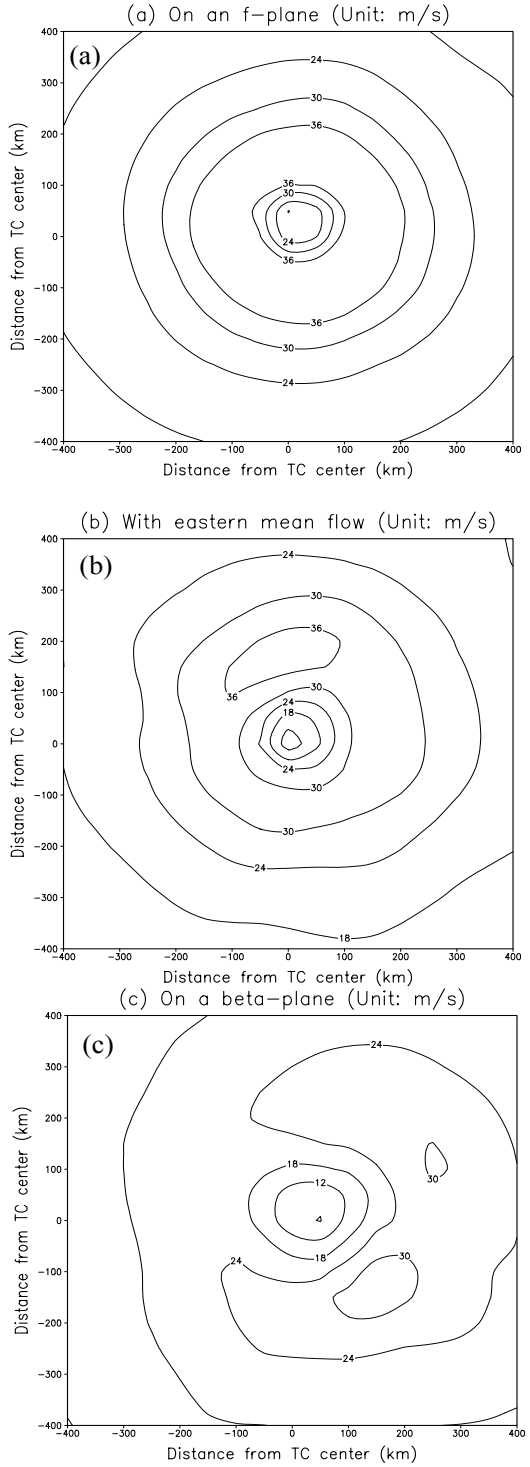

Fig. 2. Surface wind isotachs (Units: $\mathrm{m\,s^{-1}}$) at 48 h in the experiments of (a) on an f-plane, (b) with a uniform current environment and (c) on a β-plane. (Contour interval: $6\ \mathrm{m\,s^{-1}}$).

the column of rising air is also larger. Note, however, that the eye radii are similar. Second, an obvious asymmetry exists in the magnitude of the vertical motion in the easterly flow simulation with strong rising motion to the west, the difference between the two sides reaching $6\times10^{-4}\ \mathrm{hPa\,s^{-1}}$ at the upper levels. On the other hand, the magnitude of the vertical motion in the f-plane case is almost the same across the TC center. This asymmetry of vertical motion is even more significant in the β-plane case. The rising motion is much broader and stronger to the west. These results suggest that in the presence of a uniform flow or on a β-plane, the convective activity of a TC is not symmetric. This has implications for the intensity of the TCs. A detailed discussion of this point together with the subsidence in the eye will be discussed in the next section.

3.3 *Warm core*

Based on hydrostatic balance, the TC intensity must be related to the magnitude of the warm core. Indeed, a positive correlation exists between this magnitude and TC intensity. For a TC on an f-plane, the warm core has a maximum temperature anomaly of 16.4°C after 48 h of integration (Fig. 3). The corresponding anomalies for the easterly flow and β-plane cases are 15.4°C and 14.1°C respectively. Note also the east-west asymmetry of the warm core in these two cases, especially for the β-plane experiment. In addition, the width of the warm core is also different. For example, on an f-plane, the diameter of the 6°C isotherm is about 450 km but it is about 700 and 750 km in the easterly flow and β-plane cases respectively.

In summary, the presence of an easterly uniform flow or β-effect can reduce the rate of TC intensification. While these results generally agree with those from previous studies (e.g., Madala and Piacsek 1975; DeMaria and Schubert, 1984; Khain, 1988; Peng et al., 1999), they show a number of important features that may provide explanations of the reduction in the intensification rate.

4. Diagnostics around the eye region

4.1 *Subsidence in the eye*

In general, the subsidence occurs in the eye in all the experiments throughout most parts of the troposphere, from about 925 hPa to the top (Fig. 4). An important exception is the β-plane experiment in which a weak rising motion occurs in the mid-upper troposphere. Note also the bimodal structure of the vertical motion profile, with maximum subsidence found in the upper and lower troposphere. That is, the strongest (weakest) subsidence occurs in the f-plane (β-plane) case. Since subsidence is only one of the terms that can contribute towards an increase in temperature, it

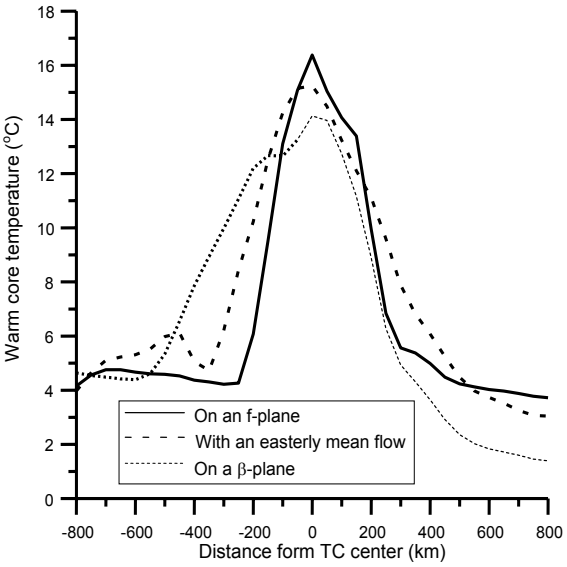

Fig. 3. Temperature anomalies on the σ=0.125 (about 210 hPa) surface in the east-west direction across the TC center at 48 h in the three experiments. (units: °C).

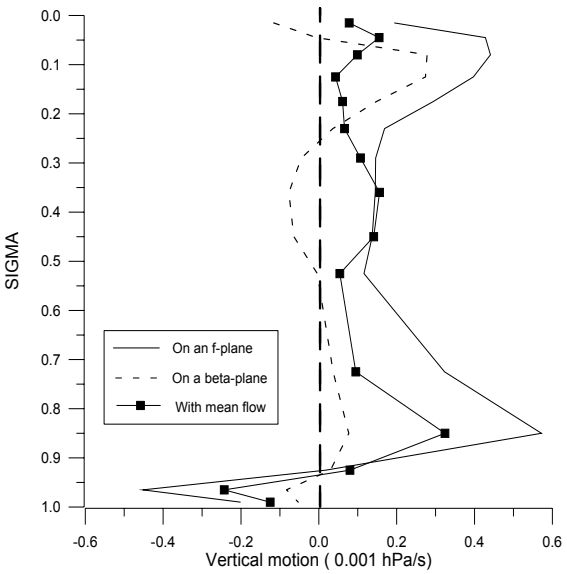

Fig. 4. Vertical motion at 48 h in the TC center in the different experiments. The thick dashed one indicates the zero line.

is necessary to examine the magnitudes of the various terms in the thermodynamic equation to identify the cause(s) of the warm core.

4.2 *Heating rates in the eye*

The heating rate can be contributed to through horizontal advection (HA), vertical advection (VA), adiabatic heating (AH), and diabatic heating (Q). An examination of these four terms indicate that the VA and Q terms are generally an order of magnitude smaller in the eye in all the experiments and can therefore be neglected.

In the f-plane and the easterly-flow simulations, the HA term is smaller and the heating is dominated by subsidence (adiabatic) warming. Consistent with the results in the previous sub-section, the magnitude of this heating is larger in the f-plane case. However, in the β-plane experiment, the magnitude of the HA term is comparable to the AH term but opposite in sign. Thus, the net warming is much smaller. In fact, a cooling occurs at about 300 hPa due to a large negative HA. An examination of the flow shows an easterly flow across the TC center (not shown). This is consistent with the temperature profile shown in Fig. 3. An alternative in explaining this negative heating rate may be in how the terms are calculated. Since the TC center intensity is determined by the MSLP, a tilting of the vortex would yield a different result. Indeed, in this simulation, the vortex begins to tilt southward at σ=0.23 (about 300 hPa), which is exactly where the negative heating occurs. Thus, the vortex tilt results in a heating rate decrease, and hence reducing the warming of the core. The tilting of the vortex is likely related to a differential β-effect at different levels (Carr and Elsberry, 1995) since no tilt is found in the other two experiments. However, since this study is focused on intensity change, no further investigation of the reason for this tilt was made.

4.3 *Upper-level divergence*

Since the strongest contribution to the heating is through subsidence warming at the upper levels, it would be of interest to examine the divergence field at these levels. The upper-level flow in the f-plane simulation is largely symmetric and anticyclonic (figure not shown). The asymmetric structure observed here is probably caused by the inertial instability and the upper boundary condition and should not be confused with that introduced by other effects. In the easterly flow and β-plane cases, the divergence field is highly asymmetric, which suggests that the convection and the corresponding vertical motion should also be asymmetric. The latter has been shown to be the case in the last section and a similar pattern is observed in the convection (not shown).

A more important result is the upper level convergence at the TC center because it is directly related to the subsidence there. In the f-plane case, the divergence at the TC center is less than -2×10^{-4} s^{-1}. On the other hand, in the experiment with an easterly flow, the magnitude of the convergence in the TC eye area is much smaller. In the β-plane experiment, the area of the convergence is even smaller.

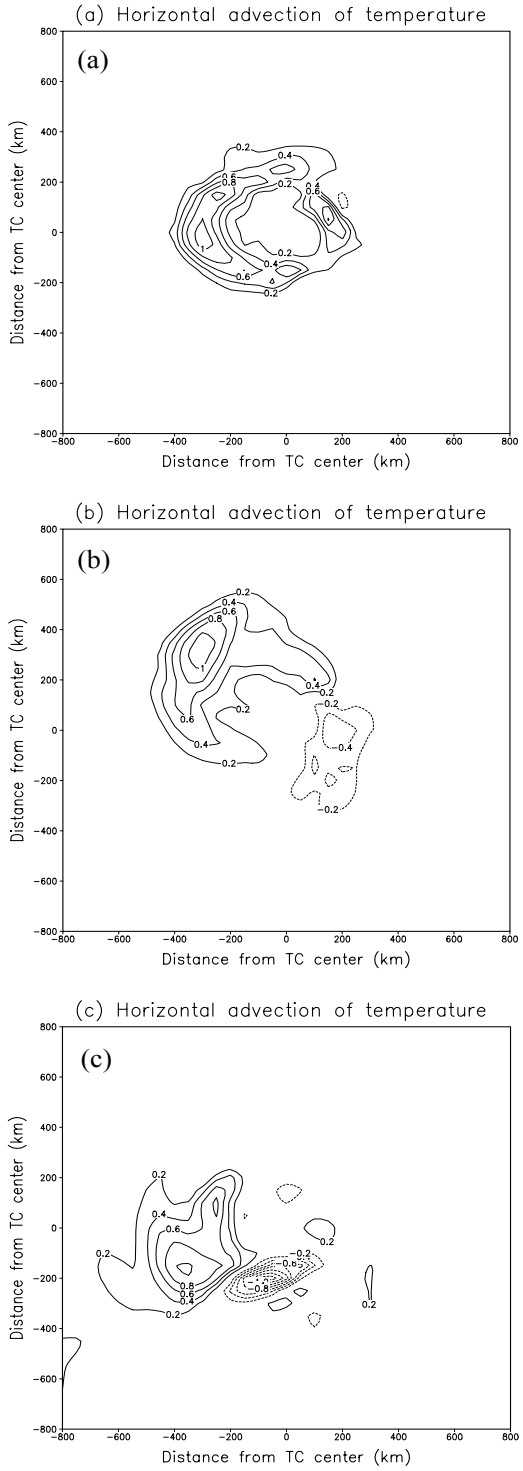

Fig. 5. Horizontal temperature advection on the σ=0.08 (about 170 hPa) surface at 48 h in the experiments of (a) on an f-plane, (b) with an easterly flow, and (c) on a β-plane. Units: 10^{-3} K s^{-1}. Interval: 0.2$\times$ 10^{-4} K s^{-1}.

These results suggest that symmetric convection would result in symmetric convergence in the eye area, and subsequently stronger subsidence. If the convection is asymmetric, the subsidence tends to be weaker.

4.4 *Heating terms around the eye*

Although adiabatic warming is the dominant term in the thermodynamic equation at the eye, this would probably not be the case in the eyewall region. Therefore, it is of interest to examine the horizontal distribution of HA, Q, and AH around the eye.

4.4.1 *Horizontal advection* (*HA*)

On an f-plane, the HA distribution on the σ=0.08 (about 170 hPa) surface at 48 h has a fairly symmetric structure (Fig. 5a) around the TC center. But in the experiment with an easterly flow, the advection shows a highly asymmetric structure. The positive and negative HA are separated, with the positive (negative) area located to the northwest (southeast) of the TC (Fig. 5b). The magnitude of the positive HA is also larger. This distribution of HA indicates that the role of HA is to cause a temperature increase to the northwest of the TC. While the distribution of HA in the β-plane experiment also shows an asymmetric structure (Fig. 5c), the maximum positive (negative) HA is to the southwest (south) of the TC.

4.4.2 *Diabatic heating* (*Q*)

As expected, the maximum latent heat release occurs near the eye in the f-plane experiment (Fig. 6a). But in the presence of an easterly flow, a long and narrow band of Q is found to the west of the TC (Fig. 6b). This indicates that the convective activity has been separated from the TC center due to the easterly flow. The magnitude of Q near the TC center is also smaller than that in the f-plane experiment. A similar situation occurs in the β-plane simulation except now that the band of Q swings around to the north of the TC (Fig. 6c). Therefore, the latent heat release is not symmetric in these two cases.

4.4.3 *Adiabatic heating* (*AH*)

On an f-plane, negative (positive) heating is found around (within) the eye area due to rising (sinking) motion (Fig. 7a). The negative heating rate has a fairly symmetric structure. But in the experiment with an easterly flow, the negative AH extends to the northwest of the TC (Fig. 7b). Consistent with the vertical motion profile, the positive AH in the core is weaker than that in the f-plane simulation. The AH distribution in the β-plane case is even more asymmetric (Fig. 7c). The eye structure is not well defined.

4.4.4 *Total heating*

The following observations can be made when the three heating terms are combined in each of the three experiments. In the f-plane simulation, the maximum heating clusters around the TC center (Fig. 8a). In

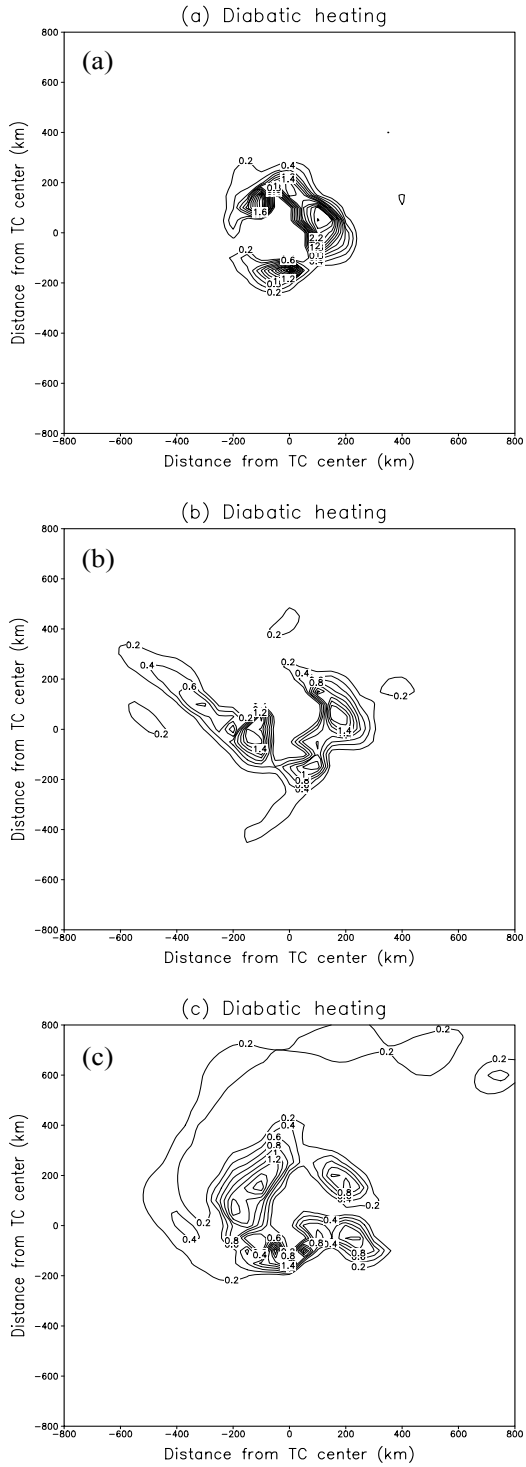

Fig. 6. Same as Fig. 5 but for the adiabatic heating.

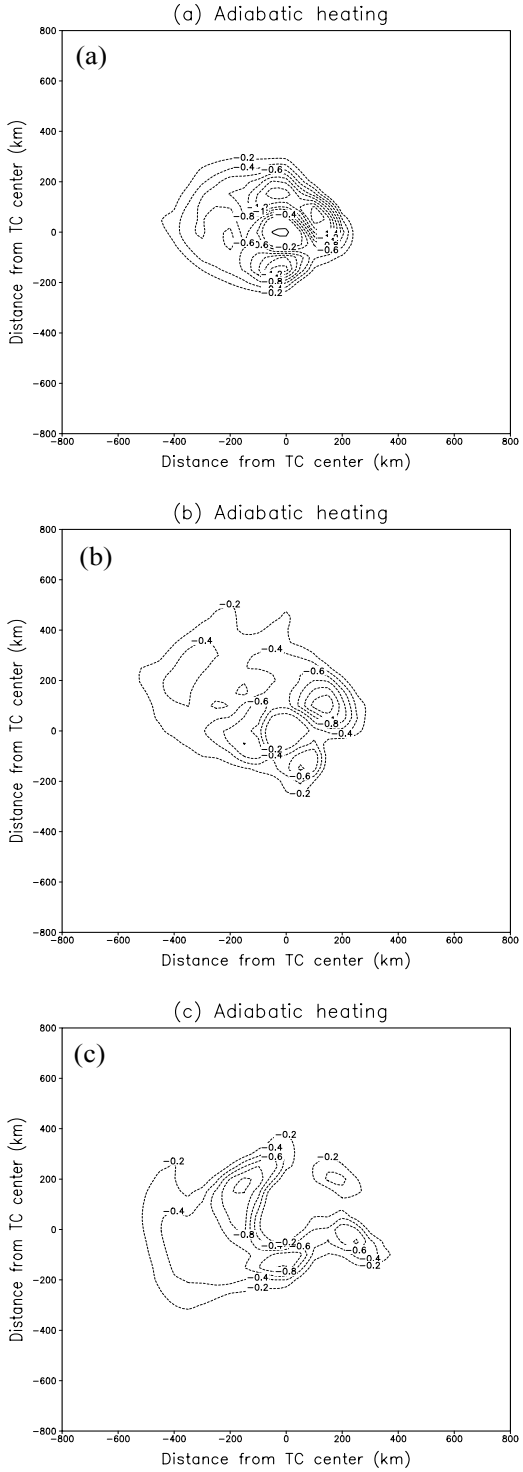

Fig. 7. Same as Fig. 5 but for the adiabatic heating.

the presence of an easterly flow, the largest positive heating rate occurs in the northwest quadrant of the TC (Fig. 8b). On a β-plane, the maximum heating is also displaced from the TC center but to the southwest, west, and north of the TC (Fig. 8c). The displacement of the heating away from the TC center in the easterly flow and β-plane experiments is mostly caused by the HA although Q also contributes signif-

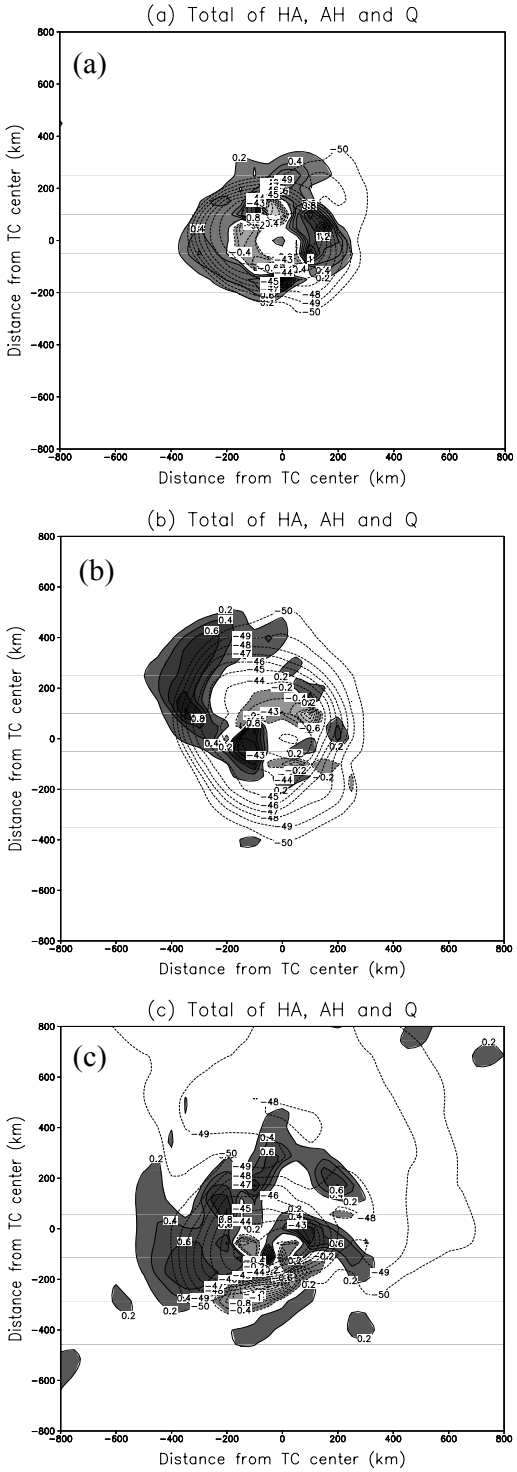

Fig. 8. Same as Fig. 5 but for the total of horizontal advection, and the adiabatic and adiabatic heating terms. The dashed line without shaded indicate the temperature (Units: 1°C; Contour interval: 1°C).

icantly in the latter. These net heating distributions explain why the TC on an f-plane is the most intense since the heating can be concentrated near the center so that maximum warming can be realized. Hydrostatic balance then dictates that the MSLP has to be the lowest among the three cases.

5. Angular momentum fluxes

5.1 *Basic formulation*

Many previous studies have examined TC intensity change from the angular momentum (AM) point of view. Since intensification is equivalent to a spinup of the TC circulation, an import of AM should be expected. Pfeffer and Challa (1981) have shown that asymmetric inward transport of AM correlates with intensification based on composite data. Holland and Merrill (1984) also obtained similar results from a simple theoretical model. They further pointed out that an export of anticyclonic AM, which occurs at the upper levels, is equivalent to an import of cyclonic AM, which would cause a TC to intensify. Thus, it would be of interest to study the angular momentum fluxes from the present model integrations and see if the same physical reasoning can be applied to explain the differences in intensification rates between the different experiments.

The following diagnostic framework follows that of Chan and Kwok (1999). The absolute angular momentum m is defined as

$$m = vr + \frac{1}{2}fr^2 \,, \tag{1}$$

where v is the tangential wind, r the radius, and f the Coriolis parameter. To study the various contributions to the changes in AM, the wind components are separated into the symmetric and asymmetric parts (denoted by an overbar and a prime, respectively). Thus, the two wind components can be written as

$$u = \bar{u} + u' \qquad v = \bar{v} + v'$$

where u is the radial component.

The AM flux $M(r)$ across a circle centered on the TC at radius r is given by

$$M(r) = \frac{\int_0^{2\pi} \left(vr + \dfrac{fr^2}{2}\right) urd\theta}{\int_0^{2\pi} rd\theta} \,, \tag{2}$$

so that after substitution,

$$M(r) = r\bar{u}\bar{v} + r\overline{u'v'} + \frac{f_0 r^2 \bar{u}}{2} + \frac{r^2\overline{fu'}}{2} \,, \tag{3}$$

where the overbar indicates an azimuthal average.

The AM transport can therefore be contributed to by four processes, as indicated on the right-hand side of (3), namely, the symmetric relative angular momentum (RAM) flux, the asymmetric or eddy RAM flux, the symmetric Coriolis torque, and the asymmetric

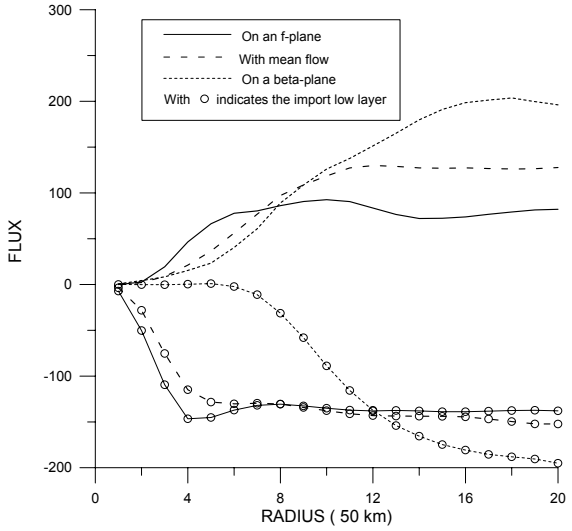

Fig. 9. Total angular momentum flux at the on upper (about 140 hPa, without symbols) and lower (about 950 hPa, with symbols) levels at 48 h in the f-plane (solid line), easterly flow (long dashed line), and β-plane (short dashed line) experiments. Units: 10^6 m^3 s^{-2}.

or eddy Coriolis torque. Adding the first and third (second and fourth) terms gives the total symmetric (asymmetric) flux. In the present study, the fluxes are calculated from the symmetric and asymmetric radial and tangential winds derived from the model output.

5.2 *Results from the f-plane experiment*

As expected, the total AM flux at the lower level (σ=0.965, about 950 hPa) is negative (i.e., import), which is contributed to almost exclusively by the symmetric import. This import reaches a maximum at about 200 km away from the TC center. Beyond this radius, the import is almost constant. At the upper level (σ=0.045, about 140 hPa) AM is being exported, as indicated by the positive AM flux, which is mainly from the symmetric term.

5.3 *β-plane and easterly flow*

On a β-plane, the AM import at the low level is quite small within 300 km (Fig. 9). Although it increases beyond this radius and actually exceeds that in the f-plane experiment at radii greater than 600 km, the total AM import in the β-plane case is obviously smaller. On the other hand, the easterly-flow case has an AM import profile very similar to that of the f-plane experiment at the low level.

The export of AM at the upper level is the least in the f-plane experiment and largest in the β-plane case. Thus, combining the effects at the low and upper levels suggests that the largest (smallest) net import of AM occurs in the f-plane (β-plane) experiment, a result which is consistent with the rates of intensification of the TC in these experiments.

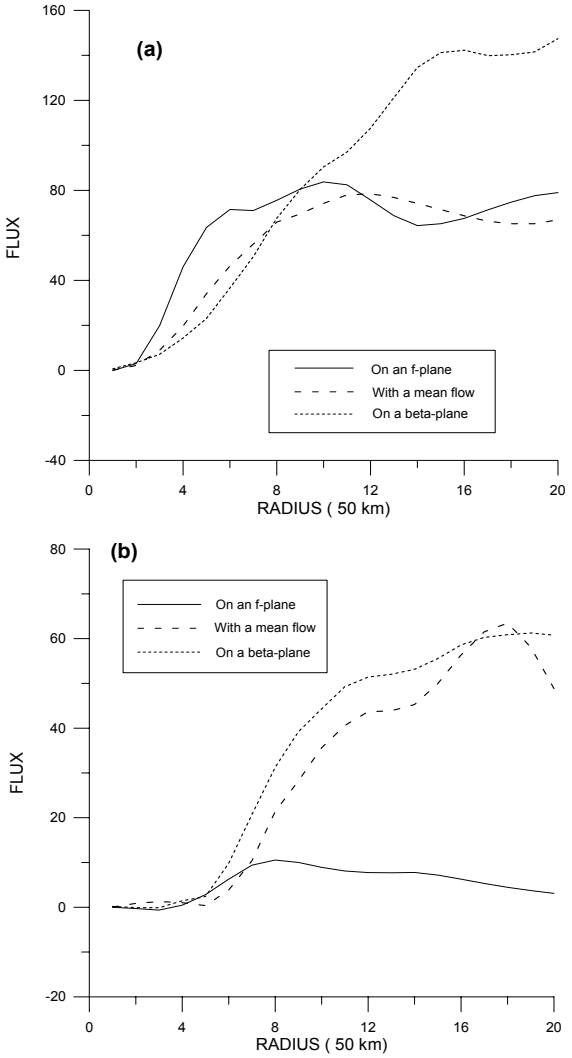

Fig. 10. Total (a) symmetric and (b) asymmetric angular momentum flux at the upper level (about 140 hPa) at 48 h in the f-plane (solid line), easterly flow (long dashed line), and β-plane (short dashed line) experiments. Note that the scales in the two figures are different. Units: 10^6 m^3 s^{-2}.

5.4 *Symmetric vs. asymmetric terms*

To understand further the relative contributions of the various processes in (3) to the AM transport, the individual terms are examined.

5.4.1 *Upper level*

The net symmetric AM flux at the upper level is almost the same for all three experiments within about 450 km (Fig. 10a). Beyond this radius, the export of AM in the β-plane experiment increases significantly. The behavior of the net asymmetric AM flux is also similar among the three cases (Fig. 10b). However, while this term remains small in the f-plane experiment due to the fairly symmetric structure of the TC,

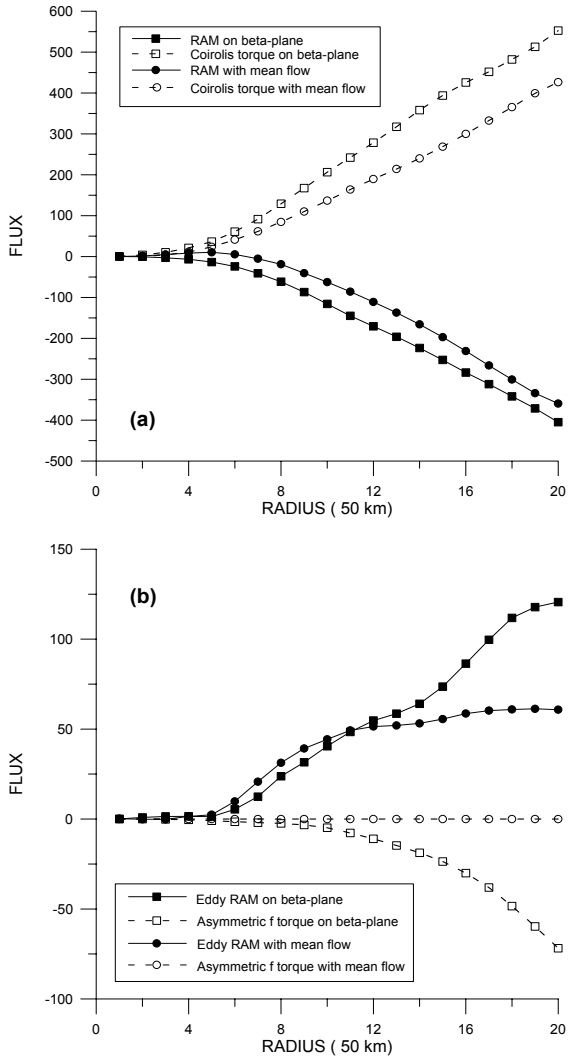

Fig. 11. (a) Symmetric and (b) asymmetric RAM (solid line) and Coirolis torque (dashed line) flux at the upper level (about 140 hPa) at 48 h in the f-plane (with the box symbol) and easterly flow (with the circle symbol) experiments. Units: 10^6 m^3 s^{-2}.

it increases at almost the same rate in the other two experiments. Thus, while the symmetric export contributes significantly to the AM transport in all three cases, AM export is enhanced by the asymmetric flow in the easterly-flow and β-plane experiments. In addition, the symmetric export in the β-plane case is also much larger at outer radii.

A further breakdown of the symmetric terms suggests that the two cases are very similar, with a symmetric RAM import and a symmetric export due to the Coriolis torque (Fig. 11a). However, the magnitudes in the β-plane case are larger, especially in the export term, which explains why the symmetric export is larger (see Fig. 10a). The asymmetric terms, on the other hand, are quite different (Fig. 11b). For the β-plane case, AM is exported through eddy RAM transport while the eddy Coriolis torque contributes to an AM import. However, because the former term is larger, the net asymmetric transport is still an export. In the easterly flow case, the eddy RAM is the main contributor of the asymmetric AM export while the eddy Coriolis torque is negligible.

5.4.2 *Low level*

It is of interest to analyze the contribution of the low-level asymmetric AM to the TC intensity. The Coriolis torque and relative angular momentum eddy terms, as well as their total, in the low layer are shown in Fig. 12. Different from that at the upper levels, the eddy Coriolis torque produces an asymmetric AM export. Within 600 km from the TC center, the eddy asymmetric terms of relative angular momentum also show an export feature.

6. Summary and discussion

6.1 *Summary*

A limited-area primitive equation model is used to study the role of the β-effect and uniform current on the change in TC intensity. On an f-plane, the effect of a uniform flow is to reduce the rate of intensification, without regard to the direction of the flow. The intensification rate is also reduced when the TC is on a β-plane. While these results are consistent with those from previous studies (e.g., Peng et al., 1999), detailed diagnoses are made to understand the causes of such changes in the rate of intensification.

Firstly, in the f-plane simulation, the TC structure is fairly symmetric. Asymmetries are found both in the horizontal and the vertical in the presence of a mean flow, and in the β-plane simulation. The magnitude of the warm core also has a close relationship with the TC intensity. The TC intensity is higher if the temperature anomaly at the center is larger, and if the horizontal temperature gradient of the warm core is stronger, which is the case in the f-plane simulation.

This large magnitude of the warm core is mainly due to strong subsidence warming in the eye. The symmetric convection, and hence convergence, is found to be the cause of this subsidence. On the β-plane, the horizontal advection of temperature partly cancels the adiabatic heating, and thus the warming of the core is less. Such an advection may be the result of the differential β-effect. Although to a lesser extent, the convection in the uniform flow case is sheared downstream and hence the net amount of warming is also less compared with that without a uniform flow.

From a dynamical point of view, while angular momentum (AM) import is found in all three cases, the

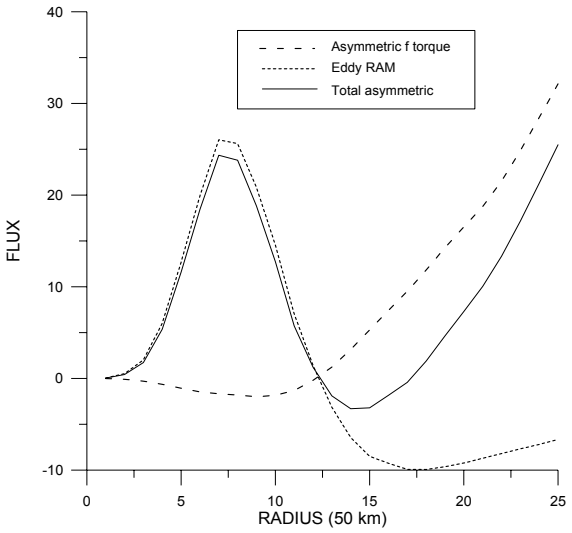

Fig. 12. Asymmetric angular momentum flux at the low level (about 950 hPa) at 48 h in the β-plane experiment. Short (long) dashed line indicates the asymmetric eddy (Coriolis torque) term. The solid line is the sum of the two. Units: 10^6 m^3 s^{-2}.

asymmetric AM flux at the upper levels is much larger in the β-plane or uniform flow experiment than in the f-plane simulation. This is again related to the asymmetry of the vortex.

6.2 *Discussion*

Although the simulations here are very simple, the results point to a very fundamental concept in the rate of TC intensification, namely the degree of asymmetry. Because in most cases, the TC would be embedded in a steering flow and obviously on a spherical earth, the presence of asymmetry is therefore the norm. Therefore, unless the environmental flow has such a configuration as to make the convection and the net flow relatively symmetric, the rate of intensification would be less than expected from the ideal case, assuming other conditions (such as those over the ocean) remain the same. In other words, one of the reasons why most TCs cannot attain their maximum possible intensity is the presence of asymmetry. The higher the asymmetry is, the smaller the intensification rate is. Of course, this statement needs to be verified by examining TCs with different rates of intensification.

Nevertheless, the diagnoses presented in this paper provide the physical mechanisms (dynamic and thermodynamic) that are responsible for the reduction in the rate of intensification in the presence of a uniform flow or for a TC on a β-plane. Such mechanisms need to be explored further when the TC is under a vertical or horizontal shear. The results of such a study will be reported in a separate paper.

Acknowledgments. This work was sponsored by the National Natural Science Foundation of China under Grant Nos. 49975014, 40275018, and 40333025. Part of the computations was completed during the first author's visit to the City University of Hong Kong (CityU) through the sponsorship of various research grants of CityU.

REFERENCES

Anthes, R. A., 1977: A cumulus parameterization scheme utilizing a one-dimensional cloud model. *Mon. Wea. Rev.*, **105**, 270–286.

Anthes, R. A., E. -Y. Hise, and Y.-H. Kuo, 1987: Description of the Penn State/NCAR mesoscale Model Version 4 (MM4). NCAR Tech. Note NCAR/TN-282, National Center for Atmospheric Research, Boulder, Colorado, 66pp.

Bender, M. A., 1997: The effect of relative flow on the asymmetric structure in the interior of hurricanes. *J. Atmos. Sci.*, **54**, 703–724.

Brown, J., and K. Campana, 1978: An economical time-differencing system for numerical weather prediction. *Mon. Wea. Rev.*, **106**, 1125–1136.

Carr, Lester E., Elsberry, and L. Russell, 1995: Monsoonal interactions leading to sudden tropical cyclone track changes. *Mon. Wea. Rev.,* **123**, 265–290.

Chan, J. C.-L., and R. H.-F. Kwok, 1999: Tropical cyclone genesis in a global numerical weather prediction model. *Mon. Wea. Rev.*, **127**, 611–624.

Chan, J. C.-L., Y.-H. Duan, and L. K. Shay, 2001: The change in tropical cyclone intensity from a simple ocean/atmosphere model. *J. Atmos. Sci.*, **58**, 154–172.

Deardorff, J. W., 1972: Parameterization of the planetary boundary layer for use in general circulation model. *Mon. Wea. Rev.*, **100**, 93–106.

DeMaria, M., and W. H. Schubert, 1984: Experiment with a spectral tropical cyclone model. *J. Atmos. Sci.*, **41**, 901–924.

DeMaria, M., 1996: The effect of vertical shear on tropical cyclone intensity change. *J. Atmos. Sci.*, **53**, 2076–2087.

Elsberry, R. L., G. J. Holland, H. Gerrish, M. DeMaria, C. P. Guard, and K. Emanuel, 1992: Is there any hope for tropical cyclone intensity prediction? —A panel discussion. *Bull. Amer. Meteor. Soc.*, **73**, 264–275.

Frank, W. M., and E. A. Ritchie, 2001: Effects of vertical wind shear on hurricane intensity and structure. *Mon. Wea. Rev.,* **129**, 2249–2269.

Fujita, T., 1952: Pressure distribution in typhoon. *Geophys. Mag.*, **23,** 437–452.

Heming, J. T., J. C. L. Chan, and A. M. Radford, 1995: A new scheme for the initialization of tropical cyclones in the UK Meteorological Office Global Model. *Meteor. Appl.*, **2,** 171–184.

Hodur, R., 1997: The Naval Research Laboratory's coupled ocean/atmosphere mesoscale prediction system (COAMPS). *Mon. Wea. Rev.*, **125**, 1414–1430.

Holland, G. J., and R. T. Merrill, 1984: On the dynamics of tropical cyclone structural changes. *Quant. J. Roy. Meteor. Soc.*, **110,** 723–745.

Holland, G., and Y.-Q. Wang, 1999: What limits tropical cyclone intensity? Preprints, 23rd Conference on Hurricanes and Tropical Meteorology, 10–15 January, Dallas, Texas, Amer. Meteor. Soc., 955–958.

Jones, S. C., 1995: The evolution of vortices in vertical shear. I: Initially barotropic vortices. *Quart. J. Roy. Meteor. Soc.,* **121**, 821–851.

Khain, A. P., 1988: A three-dimensional numerical model of a tropical cyclone with allowance for the beta-effect. *Izv. Acad. Sci. USSR. Atmos. Oceanic Phys.*, **24**(4), 266–271.

Kuo, H. -L., 1974: Further studies of the parameterization of the influence of cumulus convection on large-scale flow. *J. Atmos. Sci.*, **31**, 1232–1240.

Kurihara, Y., M. A. Bender, and R. J. Ross, 1993: An initial scheme of hurricane model by vortex specification. *Mon. Wea. Rev.*, **121**, 2030–2045.

Madala, R. V., and S. A. Piacsek, 1975: Numerical simulation of asymmetric hurricanes on a β-plane with vertical shear. *Tellus*, **27**, 453–468.

Peng, S. M., B.-F. Jeng, and R. T. Williams, 1999: A numerical study on tropical cyclone intensification. Part I: Beta effect and mean flow effect. *J. Atmos. Sci.,* **56**, 1404–1423.

Pfeffer, R. L., and C. Malakondayya. 1981: A numerical study of the role of eddy fluxes of momentum in the development of Atlantic hurricanes**.** *J. Atmos. Sci.,* **38**, 2393–2398

Ritchie, E. A., and R. L. Elsberry, 2001: Simulations of the transformation stage of the extratropical transition of tropical cyclone. *Mon. Wea. Rev.*, **129**, 1462–1480.

Shapiro, L. J., 1992: Hurricane vortex motion and evolution in a three-layer model. *J. Atmos. Sci.*, **49**, 140–153.